

Supercritical Fluid Processing of Thermally Stable Mesoporous Titania Thin Films with Enhanced Photocatalytic Activity

Kaixue Wang,[†] Baodian Yao,[‡] Michael A. Morris,[†] and Justin D. Holmes^{*,†}

Department of Chemistry, Materials Section and Supercritical Fluid Centre, University College Cork, Cork, Ireland and Department of Chemistry, Fudan University, Shanghai, 200433, P. R. China

Received April 22, 2005. Revised Manuscript Received July 18, 2005

Employing triblock copolymers as structural directing agents, high-quality mesostructured titania thin films have been prepared on silicon substrates by spin coating. Post-treatment of the films in supercritical carbon dioxide, in the presence of small amounts of either tetraisopropoxide, tetramethoxysilane, or other precursors, greatly improved the thermal stability of the mesoporous coatings without affecting their optical transparency or integrity. Nanosized anatase crystallites formed within the mesostructured walls, during the supercritical fluid treatment and calcination, prevented unidirectional contraction of the films and collapse of the pore walls at the high temperatures employed. In addition, the post-treated mesoporous titania films exhibited high photocatalytic efficiency in the degradation of waste organic compounds.

Introduction

Since the discovery of periodic mesoporous silicas by Mobil scientists in 1992,¹ a great deal of effort has focused on the preparation of mesoporous materials for a wide range of applications which include catalysis, ion-exchange, and host-guest chemistry.^{2,3} In addition, the original method for forming mesoporous silicas, based on the self-assembly between alkyltrimethylammonium surfactants and inorganic precursors under basic conditions, has been extended to a wide range of surfactants and pH conditions, leading to the discovery of new mesoporous phases with a variety of mesoscale symmetries.⁴

Crystalline non-silicate mesoporous metal oxide materials, which possess both ordered arrays of mesopores and a periodic atomic lattice, are potential candidates for applications such as battery electrodes,⁵ fuel cells,⁶ optoelectronic devices,⁷ photovoltaic devices,⁸ and photocatalysis⁹ due to

their variable oxidation states and unusual magnetic, electronic, and optical properties compared to silicates. Recently, the templating approach used for producing mesoporous silicate films has been extended to the formation of non-silica mesoporous materials.¹⁰ A variety of templates, such as alkyl phosphate anionic surfactants,¹¹ quaternary ammonium cationic templates,^{12b–c,13} primary amines,¹⁴ and poly(ethylene oxide)-based surfactants,^{12a,15a–f,16,17} have been used to manipulate the pore structures of a number of mesoporous metal oxides such as ZrO₂,¹² MnO₂,¹³ TiO₂,¹⁵ CeO₂,¹⁶ SnO₂,¹⁷ Nb₂O₅,¹⁸ HfO₂,¹⁹ Ta₂O₅,²⁰ WO₃,²¹ and

* To whom correspondence should be addressed. Phone: +353 (0)21 4903608. Fax: +353 (0)21 4274097. E-mail: j.holmes@ucc.ie.

[†] University College Cork.

[‡] Fudan University.

- (1) Kresge, C. T.; Leonowicz, M. E.; Roth, W. J.; Vartuli, J. C.; Breck, J. S. *Nature* **1992**, *359*, 710.
- (2) Corma, A. *Chem. Rev.* **1997**, *97*, 2373.
- (3) Scott, B. J.; Wirnsberger, G.; Stucky, G. D. *Chem. Mater.* **2001**, *13*, 3140.
- (4) Zhao, D.; Feng, J.; Huo, Q.; Melosh, N.; Fredrichson, G. H.; Chmelka, B. F.; Stucky, G. D. *Science* **1998**, *279*, 548. (b) Zhao, D.; Huo, Q.; Feng, J.; Chmelka, B. F.; Stucky, G. D. *J. Am. Chem. Soc.* **1998**, *120*, 6024. (c) Tanev, P. T.; Pinnavaia, T. J. *Science* **1995**, *267*, 865. (d) Bagshaw, S. A.; Prouzet, E.; Pinnevaia, T. J. *Science* **1995**, *269*, 1242. (e) Yu, C.; Yu, Y.; Zhao, D. *Chem. Commun.* **2002**, 575.
- (5) Liu, P.; Lee, S. H.; Tracy, C. W.; Yan, Y.; Turner, J. A. *Adv. Mater.* **2002**, *14*, 27.
- (6) Mamak, M.; Coombs, N.; Ozin, G. *Adv. Mater.* **2000**, *12*, 198. (b) Mamak, M.; Coombs, N.; Ozin, G. *J. Am. Chem. Soc.* **2000**, *122*, 8932.
- (7) Frindell, K. L.; Bartl, M. H.; Popitsch, A.; Stucky, G. D. *Angew. Chem., Int. Ed.* **2002**, *41*, 960.
- (8) Grätzel, M. *Curr. Opin. Colloid Interface Sci.* **1999**, *4*, 314.
- (9) Takahara, Y.; Kondo, J. N.; Takata, T.; Lu, D.; Domen, K. *Chem. Mater.* **2001**, *13*, 1194.

- (10) (a) Yang, P.; Zhao, D.; Margolese, D.; Chmelka, B. F.; Stucky, G. D. *Nature* **1998**, *396*, 152. (b) Soler-Illia, G. J. de A. A.; Grosso, D.; Sanchez, C. J. *Curr. Opin. Colloid Interface Sci.* **2003**, *8*, 109.
- (11) (a) Antonelli, D. M.; Ying, J. Y. *Angew. Chem., Int. Ed. Engl.* **1995**, *34*, 2014. (b) Stone, V. F.; Davis, R. J. *Chem. Mater.* **1998**, *10*, 1468.
- (12) (a) Crepaldi, E. L.; Soler-Illia, G. J. de A. A.; Grosso, D.; Albouy, P.; Sanchez, C. *Chem. Commun.* **2001**, 1582. (b) Yuan, Z.; Vantomme, A.; Léonard, A.; Su, B. *Chem. Commun.* **2003**, 1558. (c) Suh, Y.; Lee, J.; Rhee, H. *Catal. Lett.* **2003**, *90*, 103. (d) Suh, Y.; Lee, J.; Rhee, H. *Solid State Sci.* **2003**, *5*, 995. (e) Wong, M. S.; Ying, J. Y. *Chem. Mater.* **1998**, *10*, 2067. (f) Né, F.; Testard, F.; Zemb, Th.; Grillo, I. *Langmuir* **2003**, *19*, 8503.
- (13) Tian, Z. R.; Tong, W.; Wang, J.; Duan, N.; Krishnan, V. V.; Suib, S. L. *Science* **1997**, *276*, 926.
- (14) (a) Wang, Y.; Tang, X.; Yin, L.; Huang, W.; Hacothen, Y. R.; Gedanken, A. *Adv. Mater.* **2000**, *12*, 1183. (b) Yoshitake, H.; Sugihara, T.; Tatsumi, T. *Chem. Mater.* **2002**, *14*, 1023.
- (15) (a) Crepaldi, E. L.; Soler-Illia, G. J. de A. A.; Grosso, D.; Cagnol, F.; Ribot, F.; Sanchez, C. *J. Am. Chem. Soc.* **2003**, *125*, 9770. (b) Choi, S. Y.; Mamak, M.; Coombs, N.; Chopra, N.; Ozin, G. A. *Adv. Funct. Mater.* **2004**, *14*, 335. (c) Yue, Y.; Gao, Z. *Chem. Commun.* **2000**, 1755. (d) Crepaldi, E. L.; Soler-Illia, G. J. de A. A.; Grosso, D.; Sanchez, C. *J. New J. Chem.* **2003**, *27*, 9. (e) Luo, H.; Wang, C.; Yan, Y. *Chem. Mater.* **2003**, *15*, 3841. (f) Bosc, F.; Ayrat, A.; Albouy, P.; Guizard, C. *Chem. Mater.* **2003**, *15*, 2463. (g) Soler-Illia, G. J. de A. A.; Louis, A.; Sanchez, C. *Chem. Mater.* **2002**, *14*, 750.
- (16) Lundberg, M.; Skarman, B.; Cesar, F.; Wallenberg, R. *Microporous Mesoporous Mater.* **2002**, *54*, 97.
- (17) Miyata, H.; Itoh, M.; Watanabe, M.; Noma, T. *Chem. Mater.* **2003**, *15*, 1334.
- (18) Xu, L.; Tian, B.; Kong, J.; Zhang, S.; Liu, B.; Zhao, D. *Adv. Mater.* **2003**, *15*, 1932. (b) Murray, S.; Trudeau, M.; Antonelli, D. M. *Adv. Mater.* **2000**, *18*, 1339.
- (19) Liu, P.; Liu, J.; Sayari, A. *Chem. Commun.* **1997**, 577.

GeO₂.²² However, compared with its silica counterpart, the precursors used in the preparation of non-silicate mesoporous metal oxides are relatively reactive, making it difficult to control their hydrolysis and condensation rates. Nonaqueous solvents, such as ethanol and 1-butanol, and stabilization agents including strong acids and complexing molecules, such as diethanolamine,²³ triethanolamine,^{12c,d,24} and acetyl acetone,²⁵ have been successfully employed to hinder the hydrolysis and condensation rates, allowing successful preparation of high-quality mesoporous metal oxide thin films and powders. Among the mesoporous metal oxides prepared, mesostructured TiO₂, especially in the form of thin films, is the most attractive because crystalline titania is a low-cost photocatalyst with potential application in photovoltaics, electrochromic devices, photoconductors, fuel cells, and sensors.²⁶

Many potential applications of mesoporous titania depend on the nanocrystalline nature of the pore walls. In addition to the conventional chemical and physical properties of crystals, mesoporous materials with crystalline wall structures will possess high surface areas, which are important for photocatalytic applications. However, crystallization of amorphous walls during calcination usually leads to a collapse of the well-ordered mesostructure. Furthermore, the thermal instability of mesostructured materials occurs when the crystal grain growth exceeds the wall thickness. In an attempt to increase the thermal stability of mesoporous metal oxide materials, several postsynthesis calcination methods have been developed.^{27–30} In particular, Li and co-workers²⁷ used a crystal–glass configuration as a building block to design and synthesize mesoporous nanocomposites with high thermal stability. Functional nanocrystals were used as the building blocks of ordered mesopores, and the glass phase acted both as the “glue” between nanocrystals and as a functionalizing component. However, the impurity introduced into the mesoporous wall by the glass phase might affect

the unique properties of single-component metal oxides and restrict the applications of these materials. Cassiers et al.²⁸ reported that post-treatment of uncalcined mesoporous titania powder with ammonia resulted in the formation of mesoporous crystalline titania. The mesoporous titania produced was constructed from nanosized anatase particles and thermally stable up to 600 °C. However, the ammonia treatment is not applicable to the formation of titania thin films as the basic ammonia solution deteriorates the smooth surface of silica wafers and glass slides on which the thin films are deposited. Sanchez and co-workers²⁹ reported the preparation of high-quality mesoporous TiO₂ thin films with an anatase network that could be retained with a porosity of 35% above 650 °C by applying a specific postsynthesis delayed rapid crystallization (DRC) treatment. However, calcination of the films at temperatures as high as 730 °C for approximately 20 min resulted in complete deterioration of the mesostructure. In addition, Domen et al.³⁰ obtained ordered mesoporous crystalline Nb–Ta oxide powders by filling amorphous mesoporous Nb–Ta oxide with carbon prior to crystallization at high temperatures.

Due to its high diffusivity, low interfacial tension, and excellent wetting ability,^{31,32} supercritical carbon dioxide (sc-CO₂) has the capability to carry small molecules into voids rapidly. In our laboratory ordered arrays of nanowires and nanotubes of semiconductors, metals, and metal oxides have been created within mesoporous silica and anodic aluminum oxide (AAO) using sc-CO₂ inclusion techniques.³³ In addition, Wakayama and co-workers reported the penetration of titanium tetraisopropoxide (TTIP) molecules solvated with sc-CO₂ into the mesopores of silica³⁴ and demonstrated TTIP molecules could be easily infiltrated into the mesopores with a diameter greater than 3.5 nm. Mokoya et al.³⁵ reported the use of supercritical fluids (SCFs) to graft Al into mesoporous silica (MCM-41), producing highly aluminated materials with exceptional hydrothermal stability.

Previously we used a sc-CO₂ technique, combined with a small amount of tetramethoxy silane (TMOS), to treat mesoporous titania thin films. The post-treated thin films displayed remarkable high thermal stability.³⁶ In the present work we employ our SCF processing method³⁶ to investigate the preparation of well-defined mesostructured titania thin

- (20) Antonelli, D. M.; Ying, J. Y. *Chem. Mater.* **1996**, *8*, 874. (b) Newalkar, B. L.; Komarneni, S.; Katsuki, H. *Mater. Lett.* **2002**, *57*, 444.
- (21) Baeck, S.; Choi, K.; Jaramillo, T. F.; Stucky, G. D.; McFarland, E. W. *Adv. Mater.* **2003**, *15*, 1269. (b) Badilescu, S.; Ashrit, P. V. *Solid State Ion.* **2003**, *158*, 187.
- (22) Lu, Q.; Gao, F.; Li, Y.; Zhou, Y.; Zhao, D. *Microporous Mesoporous Mater.* **2002**, *56*, 219.
- (23) Zhang, L.; Zhu, Y.; He, Y.; Li, W.; Sun, H. *Appl. Catal. B* **2003**, *40*, 287.
- (24) Cabrera, S.; Haskouri, J. El; Beltrán-Porter, A.; Beltrán-Porter, D.; Marcos, M. D.; Amorós, P. *Adv. Mater.* **1999**, *11*, 379. (b) Cabrera, S.; Haskouri, J. El; Beltrán-Porter, A.; Beltrán-Porter, D.; Marcos, M. D.; Amorós, P. *Solid State Sci.* **2000**, *2*, 513.
- (25) Yun, H.; Miyazawa, K.; Honma, I.; Zhou, H.; Kuwabara, M. *Mater. Sci. Eng.* **2003**, *23*, 487.
- (26) Hagfeldt, A.; Grätzel, M. *Chem. Rev.* **1995**, *95*, 49. (b) Gerfin, T.; Grätzel, M.; Walder, L. *Inorg. Chem.* **1997**, *44*, 3345. (c) Campus, F.; Bonhôte, P.; Grätzel, M.; Heinen, S.; Walder, L. *Sol. Energy Mater. Sol. Cells* **1999**, *56*, 281. (d) Hoffmann, M. R.; Martin, S. T.; Choi, W. Y.; Bahnemann, D. W. *Chem. Rev.* **1995**, *95*, 69. (e) Dillert, R.; Cassano, A. E.; Goslich, R.; Bahnemann, D. W. *Catal. Today* **1999**, *54*, 267. (f) Nazeeruddin, M. K.; Kay, A.; Rodicio, L.; Humphrey-Baker, R.; Muler, E.; Liska, P.; Vlachopoulos, N.; Grätzel, M. *J. Am. Chem. Soc.* **1993**, *115*, 6382.
- (27) Li, D.; Zhou, H.; Honma, I. *Nat. Mater.* **2004**, *3*, 65.
- (28) Cassiers, K.; Linssen, T.; Meynen, V.; Voort, P. Van Der; Cool, P.; Vansant, E. F. *Chem. Commun.* **2003**, 1178.
- (29) Grosso, D.; Soler-Illia, G. J. de A. A.; Crepaldi, E. L.; Cagnol, F.; Sinturel, C.; Bourgeois, A.; Brunet-Bruneau, A.; Amenitsch, H.; Albouy, P. A.; Sanchez, C. *Chem. Mater.* **2003**, *15*, 4562.
- (30) Katou, T.; Lee, B.; Lu, D.; Kondo, J. N.; Hara, M.; Domen, K. *Angew. Chem., Int. Ed.* **2003**, *42*, 2382.

- (31) McHugh, M. A.; Krukonis, V. J. *Supercritical Fluid Extraction: Principle and Practice*, 2nd ed.; Butterworth-Heinemann: Boston, 1994. (b) Johnston, K. P.; Shah, P. S. *Science* **2004**, *303*, 482. (c) Holmes, J. D.; Lyons, D. M.; Ziegler, K. J. *Chem. Eur. J.* **2003**, *9*, 2144.
- (32) Lim, K. T.; Hwang, H. S.; Ryoo, W.; Johnston, K. P. *Langmuir* **2004**, *20*, 2466.
- (33) Coleman, N. R. B.; Ryan, K. M.; Spalding, T. R.; Holmes, J. D.; Morris, M. A. *Chem. Phys. Lett.* **2001**, *343*, 1. (b) Coleman, N. R. B.; O'Sullivan, N.; Ryan, K. M.; Crowley, T. A.; Morris, M. A.; Spalding, T. R.; Steytler, D. C.; Holmes, J. D. *J. Am. Chem. Soc.* **2001**, *123*, 7010. (c) Coleman, N. R. B.; Morris, M. A.; Spalding, T. R.; Holmes, J. D. *J. Am. Chem. Soc.* **2001**, *123*, 187. (d) Crowley, T. A.; Ziegler, K. J.; Lyons, D. M.; Erts, D.; Olin, H.; Morris, M. A.; Holmes, J. D. *Chem. Mater.* **2003**, *15*, 3518. (e) Ziegler, K. J.; Harrington, P. A.; Ryan, K. M.; Crowley, T.; Holmes, J. D.; Morris, M. A. *J. Phys.: Condens. Matter* **2003**, *15*, 8303. (f) Ryan, K. M.; Erts, D.; Olin, H.; Morris, M. A.; Holmes, J. D. *J. Am. Chem. Soc.* **2003**, *125*, 6284.
- (34) Tatsuda, N.; Fukushima, Y.; Wakayama, H. *Chem. Mater.* **2004**, *16*, 1799.
- (35) O'Neil, A. S.; Mokaya, R.; Poliakov, M. *J. Am. Chem. Soc.* **2002**, *124*, 10636.
- (36) Wang, K.; Morris, M.; Holmes, J. *Chem. Mater.* **2005**, *17*, 1269.

films using triblock copolymers as structural directing agents. As confirmed by the XRD studies and transmission electron microscope (TEM) observations, the thermal stability of the titania thin films can be significantly enhanced by sc-CO_2 treatment with the presence of a very small amount of titania or silica precursor. High-angle X-ray diffraction (XRD) and high-resolution transmission electron microscopy (HRTEM) results suggest that the mesopore walls are composed of randomly aligned anatase crystallites. In addition, the photocatalytic activities of the post-treated titania films produced are reported.

Experimental Section

Preparation of the Initial Solution. For the synthesis of mesoporous titania titanium tetraisopropoxide (TTIP) was used as the inorganic source. The triblock copolymer surfactant poly(ethylene oxide)-poly(propylene oxide)-poly(ethylene oxide) ($\text{EO}_x\text{-PO}_3\text{EO}_x$), $\text{EO}_{18}\text{PO}_{58}\text{EO}_{18}$ (P104, BASF), was used as the structure directing agent. HCl solution (37 wt %) was used as a condensation inhibitor. All reagents were used without further purification. In a typical synthesis a precursor solution was prepared by slow addition of the inorganic source into an ethanolic/HCl solution containing the template with vigorous stirring. The solution with a molar composition of 1.0:0.02:2.0:35.2 TTIP:P104:HCl:EtOH was subsequently aged at room temperature for about 3 h prior to film preparation. The clear solution can be stored at room temperature in a sealed vessel for several months without obvious changes.

Film Preparation. High-quality crack-free metal oxide thin films were prepared at room temperature by spin coating. The aged solution was dropped onto a clean silicon, mica, or glass substrate and spun at 3100 rpm for 20 s. The resulting film was aged at room temperature and 60 °C for 24 h to facilitate an evaporation-induced self-assembly process³⁷ before being annealed at 150 °C for a further 48 h.

Post-treatment of the Films. In a N_2 glovebox the films were placed into a 20 mL high-pressure cell with a small amount of TTIP or TMOS (<0.02 mL). The cell was then attached to a stainless steel reservoir (60 mL) via a three-way valve. A high-pressure pump (ISCO Instruments, PA) was used to pump CO_2 (99.99%) through the reservoir into the reaction cell. The cell was pressurized to between 34.5 and 58.6 MPa with CO_2 and placed in a furnace at temperatures ranging from 30 to 100 °C. The reaction was allowed to proceed at these conditions for approximately 15 min. To study their thermal stability, treated and untreated films were calcined at various temperatures in a tube furnace for a duration of 1 h. **Warning:** High-pressure equipment such as that required for the experiments described in this paper should be equipped with a relief valve and/or a rupture disk to minimize risk or personal injury.

Characterization. X-ray diffraction (XRD) patterns were recorded in a $\theta - 2\theta$ mode on a Philips X'pert PW3710 diffractometer. The microstructure of the samples was characterized by transmission electron microscopy (TEM) (JEOL 2000EX TEM at 200 kV) and high-resolution transmission electron microscopy (HRTEM) (Philips CM200 FEG TEM at 200 kV). Samples scratched from the substrate were suspended in ethanol by sonication. Carbon-coated copper grids were used as the sample holders. To evaluate the morphology of the film surface, scanning electron

microscopy (SEM) was performed on a JEOL JSM-5510 scanning microscope operating at 10 kV.

A procedure described previously was adopted to evaluate the photocatalytic activity of the titania thin films.³⁸ A 0.02 M solution of stearic acid in methanol was first coated on the titania-coated silicon wafers by spin coating. The silicon wafer was spun at 3100 rpm for 20 s. The films were illuminated under UV light at a wavelength of 254 nm for various time intervals. The photocatalysis process was evaluated by measuring the absorbance of the C–H vibration band of stearic acid in the range from 3100 to 2700 cm^{-1} using a Bio-Rad Exculibar Series FTIR spectrometer in a diffuse reflectance mode.

Results and Discussion

Preparation of Mesoporous Titania Thin Films. In our synthesis of mesoporous TiO_2 thin films TTIP was employed as the inorganic source as it is less reactive and easier to handle than other titanium precursors, such as titanium chloride (TiCl_4) and titanium ethoxide ($\text{Ti}(\text{OEt})_4$). The dissolution of TTIP in ethanol, under strong acidic condition, leads to formation of chloro-alkoxide species, such as $\text{TiCl}_x(\text{OR})_{4-x}$ ($\text{R} = \text{C}_2\text{H}_5$ or/and C_3H_7), which are expected to limit the extended condensation that yields dense titanium-oxo species. Thus, the addition of HCl, most of which can volatilize during the aging process after film deposition, is expected to slow the disorder-to-order transformation process which occurs during the formation of an organized mesophase.³⁹ Films were prepared with different starting solutions by varying the molar ratios of HCl and the surfactant, P104. An optically transparent and homogeneous thin film (as shown in Figure 1a and c) can be developed from a solution with a molar composition of 1.0:0.02:2.0:35.2 TTIP:P104:HCl:EtOH. Water introduced with the HCl solution will inevitably have some influence on the quality of the thin film produced. TiO_2 films prepared with an HCl/TTIP ratio over 4.0 (Figure 1b) displayed dramatic color differences at locations within the films and comet-like patterns indicating different film thicknesses. This poor optical quality may be due to phase segregation as suggested by Sanchez et al. in the preparation of mesoporous zirconia thin films.^{12a} The same phenomenon can also be observed when small amounts of distilled water are added to the initial sol. Since the liquid crystal phases of the mesoporous films are rather sensitive to the relative ratios of reactants, the amount of structural directing agent, P104, also has an important influence on film quality. When the molar ratio of P104 to TTIP was greater than 0.04, cracks within the films were observed to form during the aging process, as shown by the scanning electron microscopy image in Figure 1d. The thickness of the titania films can be controlled by varying the spinning speed or/and the content of absolute ethanol in the sol without obvious deterioration of the optical quality and the mesoporous ordering of the film.

Most of the potential applications of mesoporous titania thin films are related to the formation of crystalline anatase

(37) Lu, Y.; Ganguli, R.; Drewien, C. A.; Anderson, M. T.; Brinker, C. J.; Gong, W.; Guo, Y.; Soyez, H.; Dunn, B.; Huang, M. H.; Zink, J. I. *Nature* **1997**, *389*, 364.

(38) Ammerlaan, J. A. M.; McCurby, R. J.; Hurst, S. J. International Patent WO 00/75087 A1, 2000. (b) Bosc, F.; Ayrat, A.; Albouy, P.; Guizard, C. *Chem. Mater.* **2003**, *15*, 2463.

(39) Grosso, D.; Soler-Illia, G. J. de A. A.; Babonneau, F.; Sanchez, C.; Albouy, P.; Brunet-Bruneau, A.; Balkenende, A. R. *Adv. Mater.* **2001**, *13*, 1085.

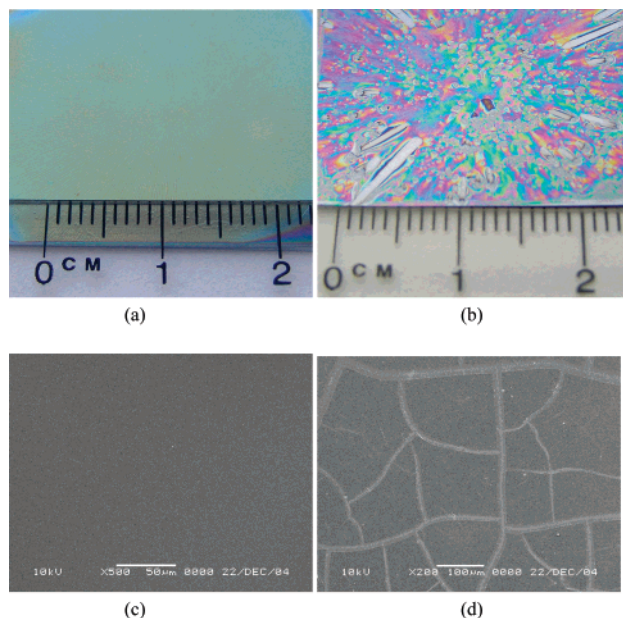


Figure 1. Optical images of mesoporous titania thin films: (a) prepared with a molar composition of 1.0:0.02:2:0:35.2 TTIP:P104:HCl:EtOH and (b) as in part a but prepared with a HCl:TTIP ratio >4.0 . SEM images (c) of the mesoporous titania film displayed in a and d thin films prepared with a molar ratio of P104:TTIP > 0.04 .

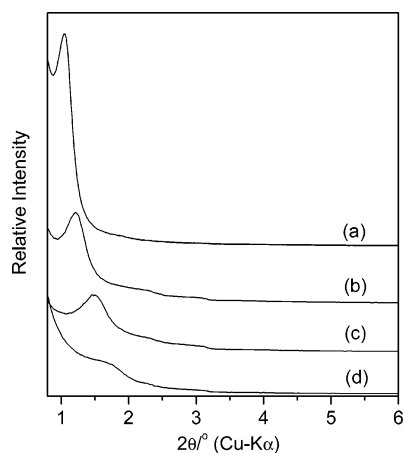


Figure 2. Low-angle XRD patterns of untreated mesoporous titania thin films calcined at (a) 150, (b) 250, (c) 350, and (d) 450 °C for a duration of 1 h each.

within the pore walls. Typically thermal treatment, which leads to transformation of the amorphous wall to a crystalline phase, is employed to form anatase crystallites. However, nucleation and growth of anatase crystallites within the mesoporous walls usually leads to collapse of the well-ordered structure. Figure 2 shows an X-ray diffraction (XRD) pattern from a mesoporous titania thin film deposited on a silicon wafer and calcined at various temperatures without $sc\text{-CO}_2$ treatment. The aging and low-temperature thermal treatments eliminate the volatile components within the films such as HCl, ethanol, and small amounts of water, allowing the progressive disorder-to-order condensation of the titania hybrid network. As observed in Figure 2, a mesoporous titania thin film without $sc\text{-CO}_2$ treatment can withstand thermal calcination up to 350 °C. The remarkable decrease in both the intensity of the (110) diffraction peak and the (110) d spacing with increasing calcination temperature implies contraction and shrinkage of the mesopores and

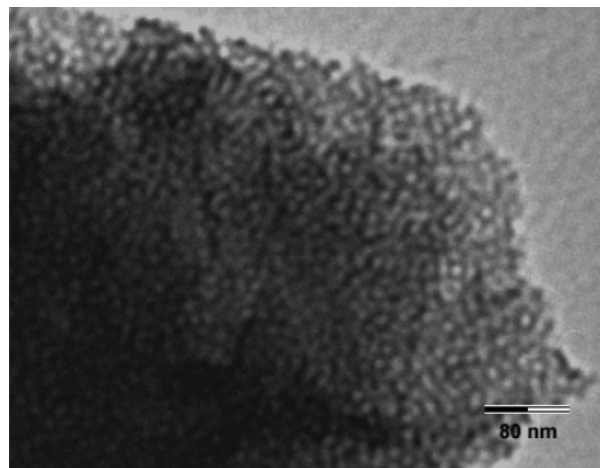


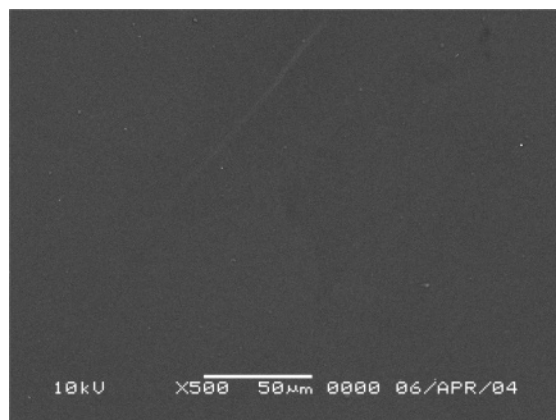
Figure 3. TEM image of an untreated mesoporous titania thin film calcined at 350 °C.

elimination of the surfactant template during the thermal treatment process. Degradation of the mesostructure is also related to formation of nanocrystalline anatase in the inorganic wall. The $d(110)$ spacing decreases from 8.2 to 5.9 nm after calcination at 350 °C, which corresponds to a 28% structural contraction. Calcination of the films at 450 °C results in almost total collapse of the ordered mesoporous structure. This result is consistent with the transmission electron microscopy (TEM) images shown in Figure 3. The TEM image of the film calcined at 350 °C shows a highly ordered mesoporous structure with pores approximately 9.0 nm in diameter. However, the TEM image of the film calcined at 450 °C shows an obvious deterioration of the mesostructure resulting from sintering of the pore walls.

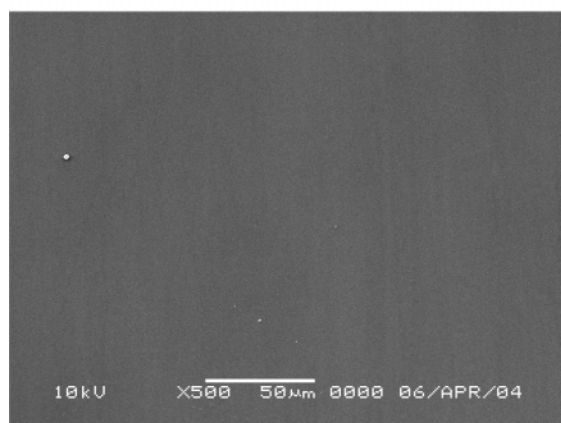
$sc\text{-CO}_2$ /TTIP Treatment. We previously reported that mesoporous titania thin films treated with $sc\text{-CO}_2$ and small amounts of tetramethoxysilane (TMOS) show improved thermal stability up to 850 °C.³⁶ Instead of TMOS, the titania precursor titanium tetraisopropoxide (TTIP) was investigated in this work. Although only very small amounts of TMOS were used in the $sc\text{-CO}_2$ treatment, Si species will inevitably penetrate into the anatase mesoporous thin films, introducing heteroatoms into its structure, which could affect its intrinsic properties. Tatsuda³⁵ reported that TTIP solubilized in $sc\text{-CO}_2$ readily penetrates the pores of mesoporous silica where it reacts with silanol groups on the surface of the pore walls. However, TTIP is relatively reactive when compared to TMOS and can easily decompose when exposed to air. Thus, the addition of small amounts of TTIP into the reaction cell was conducted in a glovebox under a N_2 atmosphere.

High-quality mesoporous titania thin films, with remarkably high thermal stability, were produced by the $sc\text{-CO}_2$ /TTIP treatment as confirmed by XRD, SEM, and TEM. SEM images of the $sc\text{-CO}_2$ /TTIP-treated titania thin films are presented in Figure 4. The surface of the films is crack free over a large scale even after calcination at temperatures over 850 °C. This result suggests that the $sc\text{-CO}_2$ /TTIP treatment and the following calcinations do not impact the surface integrity of the films.

Low-angle XRD studies of the post-treated thin films are shown in Figure 5. There is no significant change in the position of the (110) diffraction peak up to a temperature of



(a)



(b)

Figure 4. SEM images of (a) a sc-CO₂/TTIP-treated mesoporous titania thin film and (b) film a after calcination at 850 °C for 1 h.

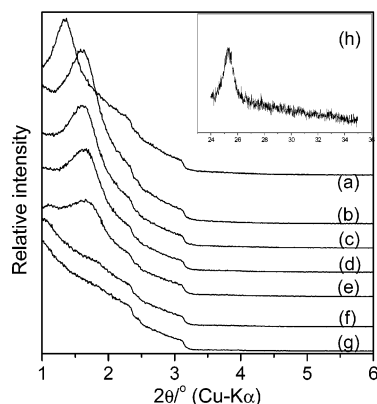
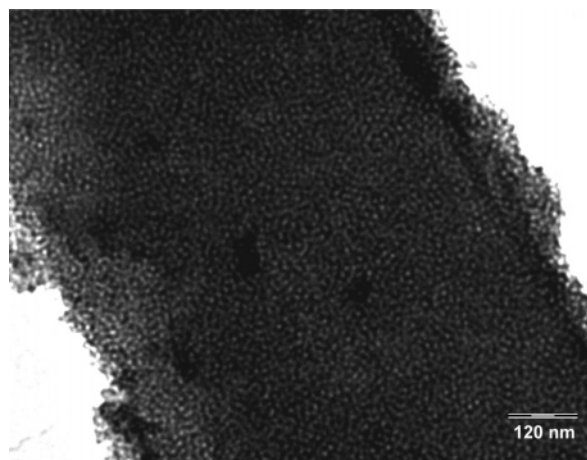
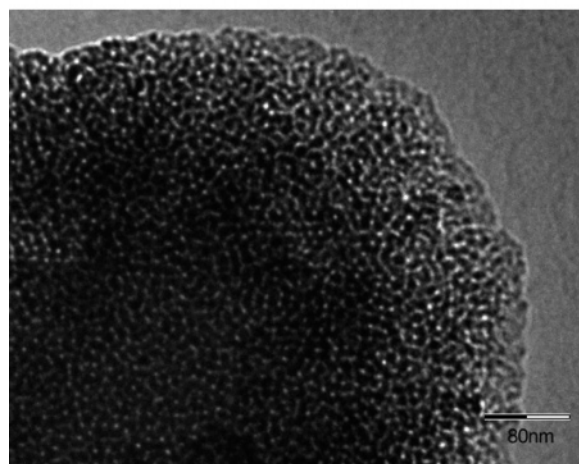


Figure 5. Low-angle XRD patterns of (a) a sc-CO₂/TTIP-treated mesoporous titania thin film and calcined at (b) 450, (c) 550, (d) 650, (e) 750, (f) 850, and (g) 950 °C. The inset (h) shows the high-angle XRD patterns of a sc-CO₂/TTIP-treated titania thin film calcined at 750 °C showing the presence of an anatase phase.

750 °C. The negligible shift of the (110) diffraction peak with increasing temperature indicates that the ordered mesoporous structure was sustained without obvious contraction during the high-temperature condensation and crystallization of the films. In addition, the width of the (110) diffraction peak did not change significantly at calcination temperatures up to 650 °C. The small variation in the peak position and width of the diffraction peaks from the thin films calcined at high temperatures indicates the high thermal stability of the mesoporous structure after sc-CO₂/TTIP treatment. A



(a)



(b)

Figure 6. TEM images of mesoporous titania thin films calcined at (a) 750 and (b) 850 °C, respectively, after sc-CO₂/TTIP treatment.

small diffraction peak does however appear at approximately 1.8° (2θ) upon calcination of the films at 850 °C for 1 h, indicating that the ordered mesostructure was preserved to some extent. Calcination of the thin films for significant time periods at temperatures over 950 °C leads to deterioration of the mesostructure. The inset shown in Figure 5 is a high-angle XRD pattern from a sc-CO₂/TTIP-treated mesoporous TiO₂ film. The obvious appearance of the broadened diffraction peak located at 25.4° (2θ) after calcination, corresponding to the (101) diffraction of anatase, suggests that the mesostructured walls of the thin films are composed of nanosized anatase crystallites.

The low-magnification TEM images shown in Figure 6 confirm the presence of mesoscale ordering of the film even after high-temperature calcination. The pore size and wall thickness of the films calcined at 750 °C are in the range between 7–9.0 and 5.0–7.0 nm, respectively. Consistent with the XRD study, the mesoporous structure of thin films calcined at a temperature of 850 °C is still preserved as seen in the TEM image. However, there is an obvious loss in the pore ordering and the pore diameter shrinks to approximately 6.0 nm. Usually the alignment of mesopores in thin films is along the surface of the substrates.^{15a} Anisotropic contraction of mesoporous titania thin films, on substrates such as glass

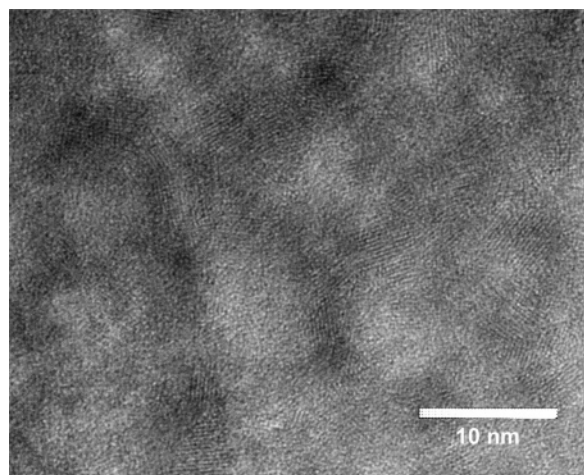


Figure 7. HRTEM image of a sc-CO₂/TTIP-treated mesoporous titania thin film following calcination at 750 °C for 1 h.

slides and silicon wafers, is usually observed during thermal treatment at temperatures above 350 °C, leading to formation of the ellipse-shaped pores.^{15b,d,39} However, as observed from the cross-sectional area by TEM studies, films treated with sc-CO₂/TTIP do not display unidirectional pore shrinkage even at temperatures above 750 °C. This result suggests that after SCF treatment the walls of the titania films are strong enough to resist anisotropic contraction typically observed with high-temperature calcination.

High-magnification TEM images of the titania films are shown in Figure 7. The anatase lattice fringe present throughout the wall structure indicates the highly crystalline nature of the films, which is in good agreement with the results from the high-angle XRD studies. The anatase crystals embedded in the mesoporous walls are oriented in a random manner which allows the nanocrystals to nucleate and grow within the limited space of the pore wall without causing destruction of the ordered mesostructures.

The experimental results suggest that as with the sc-CO₂/TMOS experiment, sc-CO₂/TTIP treatment can also greatly improve the thermal stability of mesoporous titania thin films. The mechanism by which sc-CO₂/TTIP treatment leads to thermally stable titania films is expected to be similar to that proposed for the sc-CO₂/TMOS-treated films.³⁶ Prior to post-treatment some Ti–OH and Ti–Cl groups and Ti–oxo–hydroxo oligomers exist on the surface or near surface sites on the pore walls. Due to the high penetrating power of sc-CO₂,⁴⁰ Ti species are expected to infiltrate into the mesopores of the titania films and occupy the surface and near-surface sites of the pore walls. Their reaction with the Ti–OH and Ti–Cl groups and Ti–oxo–hydroxo oligomers to form high μ -oxo connectivity will contribute to consolidation of the pore wall. Consequently, the condensed wall structure can resist any unidirectional contraction when it is subjected to high-temperature calcination and therefore exhibits high thermal stability.

Photocatalytic Properties of the Mesoporous Titania Films. There has been growing interest in the application of photocatalysis toward treatment of polluted water.⁴¹ Several

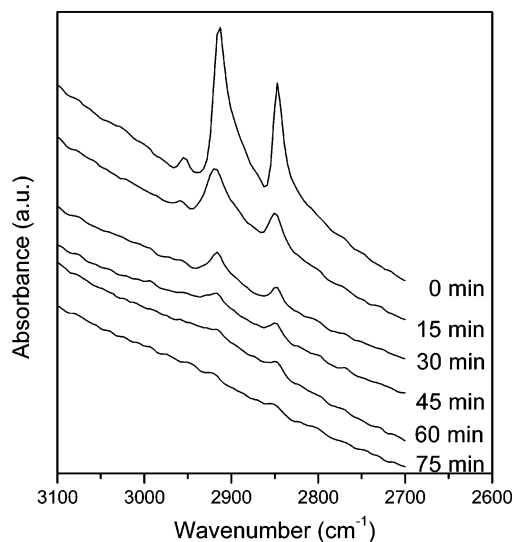


Figure 8. Disappearance of the IR peaks for stearic acid (C–H stretches at 2912 and 2847 cm⁻¹) on the surface of a sc-CO₂/TTIP-treated titania thin film after irradiation with UV light ($\lambda = 256$ nm).

semiconductors, including TiO₂, CdS, ZnO, and WO₃, have been employed as photocatalysts for the degradation of organic pollutants. Among them, TiO₂ is the most attractive semiconductor for the purification and treatment of contaminated water due to its low toxicity, photostability, and low cost. To obtain the high photocatalytic performance required for the decomposition of organic pollutants, crystalline anatase with a high surface area is required. Upon high-temperature treatment the sc-CO₂/TTIP-treated TiO₂ thin films possess a fully crystallized mesoporous wall structure up to 850 °C. Therefore, a high photocatalytic activity is expected from the films.

The photocatalytic activity of the TiO₂ thin films was evaluated based on the decomposition of stearic acid as described in the literature. Both the sc-CO₂-treated and untreated films were calcined at 550 °C for more than 1 h prior to the photocatalysis experiment. The photocatalysis process was observed by measuring the disappearance of the infrared absorbance of the C–H vibration of stearic acid at 2912 cm⁻¹. Figure 8 shows the IR spectra of stearic acid, in the wavenumber range between 3100 and 2700 cm⁻¹, as a function of time during photodegradation by sc-CO₂/TTIP-treated thin film. The progressive disappearance of the C–H vibration bands suggests that stearic acid is gradually photodegraded by the titania thin films upon illumination with UV light. After approximately 75 min the C–H peaks completely disappeared, suggesting total degradation of stearic acid.

Figure 9 shows the degradation curves for an untreated TiO₂ thin film, a sc-CO₂/TMOS-treated thin film, and sc-CO₂/TTIP-treated thin films. The decrease in the stearic acid concentration with the sc-CO₂/TTIP-treated film is consider-

(40) Pai, R. A.; Humayun, R.; Schulberg, M. T.; Sengupta, A.; Sun, J. N.; Watkins, J. J. *Science* **2004**, *303*, 507.

(41) Candal, R. J.; Zeltner, W. A.; Anderson, A. M. *Environ. Sci. Technol.* **2000**, *34*, 3443. (b) Vinodgopal, K.; Hotchandani, S.; Karnat, P. V. *J. Phys. Chem.* **1993**, *97*, 9040. (c) Leng, W. H.; Zhang, Z.; Zhang, J. Q. *J. Mol. Catal.* **2003**, *206*, 239. (d) Horikoshi, S.; Watanabe, N.; Mukae, M.; Hidaka, H.; Serpone, N. *New J. Chem.* **2001**, *25*, 999. (e) Ryu, C. S.; Kim, M.; Kim, B. *Chemosphere* **2003**, *53*, 765. (f) Zheng, S. K.; Xiang, G.; Wang, T. M.; Pan, F.; Wang, C.; Hao, W. C. *Vacuum* **2004**, *72*, 79.

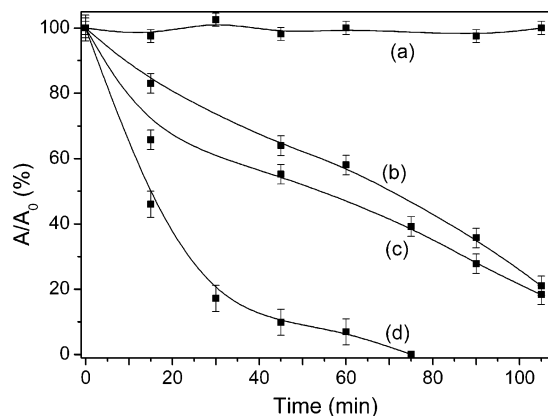


Figure 9. Evaluation of the photocatalytic activity of (a) silicon wafer, (b) mesoporous titania thin films, and the films post-treated by (c) sc-CO₂/TMOS and (d) sc-CO₂/TTIP, based on the absorbance ratio A/A_0 as a function of UV illumination time. A and A_0 are the absorbance values measured at 2912 cm⁻¹ for the UV-illuminated stearic acid layer and the initial layer without UV illumination, respectively.

ably faster compared to the untreated and sc-CO₂/TMOS-treated films. The higher efficiency can be explained by its high porosity and the presence of its highly photoactive anatase nanocrystalline structure. Without sc-CO₂ treatment calcination at temperatures above 550 °C inevitably leads to collapse of the ordered mesoporous structure and formation of rutile crystallites in the walls of the TiO₂ thin films from the transformation of anatase nanocrystals. Rutile has

a relatively low photocatalytic activity compared to anatase. Although the sc-CO₂/TMOS-treated films exhibit high porosity and anatase nanocrystallines can be observed within the walls of the treated films, the existence of a small amount of Si species within the walls deteriorates their photocatalytic ability compared to the sc-CO₂/TTIP-treated films.

Conclusion

In summary, a simple and efficient sol-gel method has been developed for the preparation of high-quality mesoporous titania thin films. Their thermal stability can be greatly enhanced from about 350 to 850 °C using a supercritical fluid post-treatment process. High-temperature calcination of the films leads to formation of nanocrystals of anatase within the pore walls without causing collapse of the mesoporous structure. The sc-CO₂/TTIP-treated titania thin films exhibit high photocatalytic activity and can be used as catalysts for the room-temperature photodegradation of organic pollutants. The SCF post-treatment is a facile and reproducible way to incorporate functional atoms into mesoporous thin films.

Acknowledgment. We acknowledge financial support from Science Foundation Ireland.

CM0508571